CdTe Quantum Dots in Ionic Liquid: Stability and Hole Scavenging in the Presence of a Sulfide Salt

ARTICLE *in* THE JOURNAL OF PHYSICAL CHEMISTRY C · JULY 2014

Impact Factor: 4.77 · DOI: 10.1021/jp507271t

6 AUTHORS, INCLUDING:

chandra sekhar
University of Hyderabad
4 PUBLICATIONS **24** CITATIONS
SEE PROFILE

Santhosh Kotni
Saveer Biotech Limited
17 PUBLICATIONS **185** CITATIONS
SEE PROFILE

Jaini Praveen Kumar
University of Hyderabad
2 PUBLICATIONS **40** CITATIONS
SEE PROFILE

Navendu Mondal
University of Hyderabad
5 PUBLICATIONS **40** CITATIONS
SEE PROFILE

THE JOURNAL OF PHYSICAL CHEMISTRY C

Article

pubs.acs.org/JPCC

CdTe Quantum Dots in Ionic Liquid: Stability and Hole Scavenging in the Presence of a Sulfide Salt

M. Chandra Sekhar, Kotni Santhosh,† Jaini Praveen Kumar, Navendu Mondal, S. Soumya, and Anunay Samanta*

School of Chemistry, University of Hyderabad, Hyderabad 500046, India

Supporting Information

ABSTRACT: The light-harvesting properties of both CdSe and CdTe nanocrystals are ideally suited for their use in quantum dot (QD)-sensitized solar cells. However, corrosion of the CdTe QD in an aqueous environment in the presence of sulfide/polysulfide electrolyte renders it unsuitable despite its better electron injection ability (compared to CdSe QD) to a large band-gap semiconductor like TiO_2. In this work, we explore the stability of a CdTe QD, which we have developed exclusively for its use in ionic liquids, in 1-butyl-3-methylimidazolium hexafluorophosphate ionic liquid in the presence of S^{2-} and investigate the hole transfer process from this photoexcited QD to S^{2-}. We not only demonstrate that an appropriate capping of the CdTe QD and use of an ionic liquid in place of the aqueous medium enhances the stability of the QD significantly in the presence of S^{2-} but also provide evidence of hole transfer from a photoexcited QD to the sulfide salt using steady-state and time-resolved emission and ultrafast transient absorption measurements.

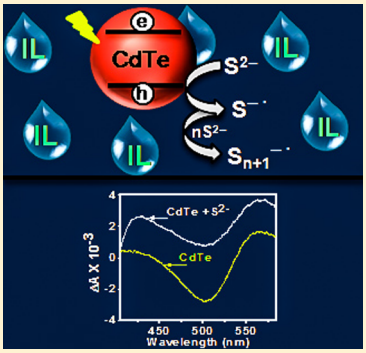

1. INTRODUCTION

Considerable attention is being paid in recent years to the photovoltaic devices to meet our ever increasing demand of energy using renewable energy sources.[1] Dye-sensitized solar cells (DSSCs) are considered to be the tools for capturing and converting solar energy into electrical energy despite their poor conversion efficiency.[2] In DSSCs, a dye molecule harvests the solar energy and injects the photogenerated electron to a large band-gap semiconductor like TiO_2 or ZnO, which subsequently transfers it to a working electrode.[2,3] Colloidal quantum-confined semiconductor nanoparticles, commonly termed as quantum dots (QDs), have become promising alternatives to the molecular dyes in solar cells because of their high molar extinction coefficient (10^4 to 10^6 M^{-1} cm^{-1} at the first exciton transition range), broad absorption, and size-dependent tunability of the band gap.[4−20] Metal chalcogenide based quantum dots, such as CdSe, CdTe, PbS, and PbSe, which have small band gaps, are considered to be ideal sensitizers for harvesting the solar energy in the visible and infrared regions.[12,21,22] The energy conversion efficiency of the quantum-dot-sensitized solar cells (QDSSCs) is mainly governed by the rates of (i) transfer of photogenerated electron to the large band-gap semiconductors like TiO_2 or ZnO and its subsequent transfer to the working electrode, and (ii) scavenging of the hole by the redox electrolyte and regeneration of the latter at the counter electrode (Scheme 1). Even though the overall power conversion efficiency (reported to be ∼6−7%)[13−15] in the QDSSCs is well below that in dye-sensitized solar cells (11%),[23] the multiple exciton generation possibility in QDs can boost the energy conversion efficiency of the QDSSCs significantly.[16,24,25] As an understanding of the dynamics of electron and hole transfer of the QDs with TiO_2 and a hole scavenger, respectively, is key to improving this efficiency, considerable importance is being given to this aspect in recent years.[17−19] Kamat and co-workers recently found that, even though the rate of electron injection to TiO_2 from CdTe

Scheme 1. Functioning of a QDSSC[a]

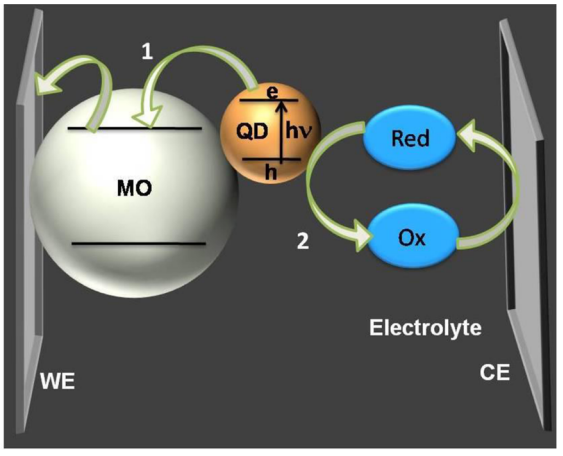

[a](1) Photoinduced electron injection to a large band-gap metal oxide (MO) and its transfer to the working electrode (WE). (2) Hole scavenging by the redox electrolyte and its regeneration at the counter electrode (CE).

Received: July 21, 2014
Revised: July 25, 2014
Published: July 25, 2014

   dx.doi.org/10.1021/jp507271t | J. Phys. Chem. C 2014, 118, 18481−18487

Chart 1

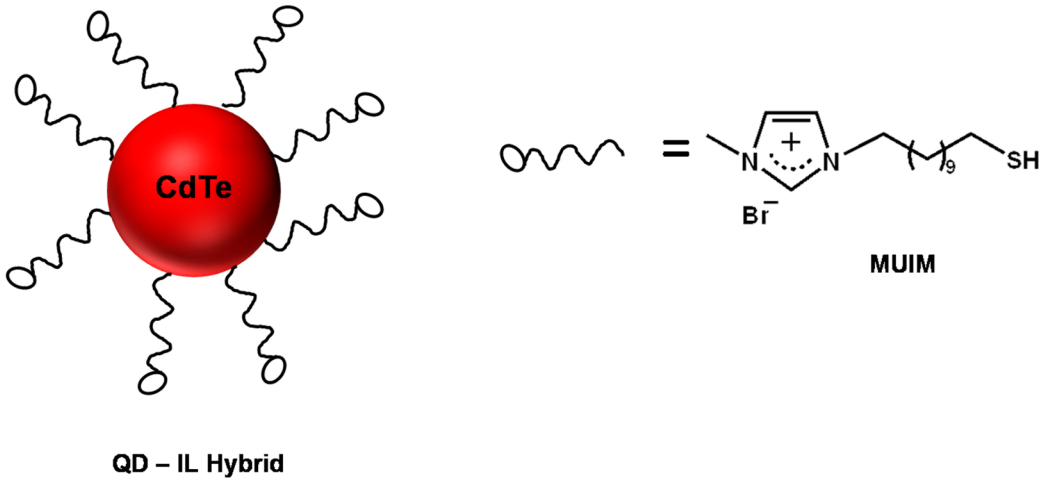

QDs is higher by an order of magnitude compared to CdSe QDs,[17] the former is unsuitable in these applications due to its degradation in the presence of a very commonly used hole scavenger, a sulfide ion, in an aqueous environment.[17,26]

This drawback of the CdTe QDs can be addressed either by employing a hole scavenger other than S^{2-} (that does not corrode the QDs) or by using a medium in which the hole transfer process is much faster than the corrosion process. Earlier attempts with redox couples such as I_3^-/I^-, ferrocene/ferrocene$^+$, and $K_4Fe(CN)_6/K_3Fe(CN)_6$ with or without KCN, however, were found to be ineffective, and rapid corrosion of CdTe QDs could not be prevented.[17] Herein, we explore the alternative strategy of finding a medium that provides enhanced stability to the QDs and at the same time allows hole scavenging by S^{2-}. It is in this context, we evaluate the suitability of an ionic liquid (IL) in place of the aqueous environment.

The ILs, which are salts comprising large ionic constituents having a melting point below 100 °C, are often regarded as better alternatives to the conventional solvents for their negligible vapor pressure, high thermal stability, and ability to dissolve a large number of inorganic and organic compounds.[27−29] High ionic conductivity, a wide electrochemical window, and low reactivity have made the ILs popular electrolytes for lithium-ion batteries and fuel cells.[30,31] ILs are also being considered as alternative media in dye/QD-sensitized solar cells.[20,32,33]

As CdSe or CdTe QDs with conventional capping agents are insoluble in ILs, it is necessary to cap these QDs with specific agents for their use in ILs. Recently, we have developed an appropriately capped CdTe QD, essentially a QD−IL hybrid (Chart 1), which dissolves both in hydrophobic and hydrophilic ILs and provides a greater stability to the QD in ILs.[34] In this work, we have employed 1-butyl-3-methylimidazolium hexafluorophosphate, [bmim][PF_6], as the IL (primarily for its excellent optical transmission properties[35]) to study the stability of this CdTe QD in the presence of S^{2-} and hole scavenging of the photoexcited QD by S^{2-} using steady-state and time-resolved fluorescence and ultrafast pump−probe measurements.

2. EXPERIMENTAL SECTION

2.1. Materials and Methods. Cadmium acetate and sodium sulfide were procured from local suppliers. Tellurium powder (Te), hexadecylamine (HDA), trioctylphosphine (TOP), 1-methylimidazole, and 11-bromoundecanethiol were procured from Aldrich. 1-Butyl-3-methylimidazolium hexafluorophosphate, [bmim][PF_6], was obtained from Kanto Chemicals. The IL was dried under vacuum for several hours before use. The solvents methanol and chloroform were purchased from Merck and distilled by reported procedures prior to use.[36] 1-Methylimidazole was distilled from KOH under reduced pressure. For optical studies in the presence of Na_2S, the required amount of a methanol solution of Na_2S was added to a solution of CdTe QDs in [bmim][PF_6], and then methanol was removed under vacuum.

2.2. Synthesis of Task-Specific CdTe QDs for Studies in ILs. The synthesis involved three steps. The first step involved preparation of CdTe QDs capped with TOP and HDA, the second step involved preparation of a specific thiol-functionalized capping agent, 1-methyl-(11-undecanethiol) imidazolium bromide salt (MUIM), for the QDs for study in ILs, and the third step involved replacement of TOP and HDA with the task-specific capping agent.

Step I: CdTe QDs capped with TOP and HDA were prepared following a reported procedure with minor modifications.[37] Briefly, $Cd(CH_3COO)_2$ (0.41 g) and Te (0.16 g) were mixed in a reagent bottle to which TOP (5 mL) was added and sonicated until a clear solution was obtained. In a two-neck round-bottom flask (RB), a mixture of HDA (5 g) and TOP (3 mL) was heated to 80 °C in an argon atmosphere, and then, the sonicated solution was injected into the RB and the temperature was slowly increased to 140 °C. When the QDs of desired size were obtained (monitored through emission), the RB was removed out of the heating mantle and allowed to cool to room temperature. To remove excess ligands, methanol was added to the reaction mixture and the precipitate was separated by centrifugation. This precipitate was dissolved in chloroform to obtain the CdTe QDs.

Step II: The task-specific capping agent, MUIM, was synthesized following a known procedure.[34] Briefly, 11-bromoundecanethiol was first added dropwise to 1-methylimidazole under an ice bath in the 1.5:1 mol ratio, and then the reaction was carried out at room temperature under a nitrogen atmosphere for 24 h. The light yellow colored solid MUIM was treated with ethyl acetate to remove the unreacted starting materials and dried under vacuum for several hours.

dx.doi.org/10.1021/jp507271t | J. Phys. Chem. C 2014, 118, 18481−18487

Step III: A $CHCl_3$ solution of MUIM (0.05 M) was added slowly to a $CHCl_3$ solution of CdTe QDs (prepared in Step I) until the particles flocculate. The precipitate was separated by centrifugation and dissolved in [bmim][PF_6] to obtain fluorescent CdTe QDs for studies in ILs.

2.3. Instrumentation. *2.3.1. Steady-State Absorption and Emission and Time-Resolved Emission Setup.* Steady-state absorption and fluorescence spectra of the samples were recorded using a UV−vis spectrophotometer (Cary 100, Varian) and a spectrofluorimeter (Fluorolog-3, Horiba Jobin Yvon), respectively. Fluorescence decay profiles were measured using a time−correlated single-photon counting spectrometer (5000, Horiba Jobin Yvon IBH) employing a Nano LED as the excitation source (439 nm, 1 MHz repetition rate, and 150 ps pulse width) and an MCP photomultiplier (Hamamatsu R3809U-50) as the detector. Additional details on this setup including the analysis of the decay curves can be found elsewhere.[38,39]

2.3.2. Femtosecond Pump−Probe Setup. The ultrafast transient absorption measurements were performed using a femtosecond time-resolved collinear pump−probe setup. The laser systems (Spectra Physics) of this setup consisted of a mode-locked Ti-sapphire oscillator (seed laser, Mai-Tai), which produced femtosecond pulses (fwhm < 100 fs, ∼2.5 W at 80 MHz) with a wide tunable range of 690−1040 nm. The seed pulse centered around 800 nm was directed to a regenerative amplifier (Spitfire Ace). The titanium sapphire rod in the amplifier was excited by a frequency-doubled Nd:YLF laser (Empower) at 527 nm. The major output (∼75%) from the amplifier (800 nm, <100 fs, 1 kHz, pulse energy ∼ 4.2 mJ) was made to pass through an optical parametric amplifier (TOPAS-Prime) to obtain a wide wavelength tuning range of 290−2600 nm. The output from TOPAS was directed to the transient absorption spectrometer (Excipro, CDP System) and used as the excitation source for the sample. The remaining (25%) portion of the amplifier output was allowed to pass through an optical delay line of 4 ns with a minimum step resolution of 1.5625 fs and then through a rotating CaF_2 crystal to generate a white light continuum (WLC). The white light was split into two parallel beams as probe and reference by using a beam splitter and then projected onto the rotating quartz sample cell. The pump and probe beams were focused onto the sample cell of 1 mm path length by maintaining an angle of less than 5° for better overlap. The transmitted probe and reference beams were directed through an optical fiber to a polychromator and then detected by a pair of photodiode arrays. The experiments were recorded with a pump energy of <1 μJ to avoid photodegradation of the CdTe.

The difference in optical density of the sample probed by WLC in the presence and absence of an excitation pump was analyzed by ExciPro software (CDP Systems). Two-photon absorption (TPA) signal of ethanol was used for the estimation of the time resolution and the "time zero". The instrumental resolution after chirp correction was found to be ∼80 fs. The overall chirp in the WLC spectrum was applied to remove the group velocity dispersion (GVD) effect from the measured data of CdTe in the IL for correct analysis. To improve the signal-to-noise ratio, we recorded the spectrum and kinetics of CdTe in the IL with a large number of averaging.

3. RESULTS AND DISCUSSION

3.1. Steady-State and Time-Resolved Experiments. The absorption and emission spectra of the CdTe QDs in [bmim][PF_6] are shown in Figure 1. The first exciton band absorption maximum of the QDs is observed at ∼510 nm and

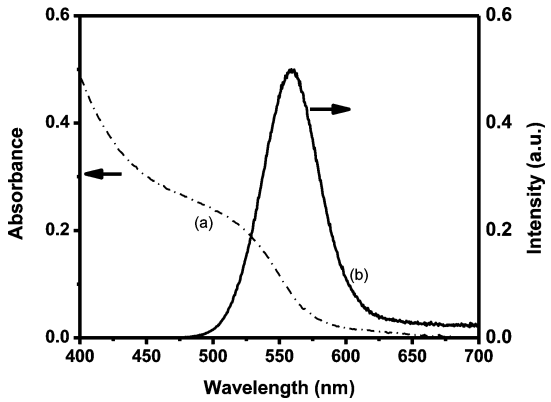

Figure 1. Absorption (a) and emission (b) spectra of CdTe QDs in [bmim][PF_6].

the emission maximum at ∼560 nm. The average size of the CdTe QDs estimated from the first exciton band maximum using Peng's equation[4] is 2.55 nm. Our attempts to determine the size of the QDs by TEM measurements were unsuccessful as clear images could not be obtained due to incomplete removal of the ionic liquid owing to its nonvolatility.

As can be seen from Figure 2, addition of Na_2S leads to slight broadening of the first exciton band of the QD in [bmim][PF_6] perhaps due to the formation of a shell of CdS resulting from the interaction of the sulfide ion with the surface Cd^{2+}.[18] The stability of the QDs in [bmim][PF_6] in the presence of the sulfide salt is evident from a comparison of the absorption spectra of the QDs at different times after addition (shown in Figure 2b). Negligible change of the spectrum in the presence of S^{2-} even after 72 h indicates no decomposition of the QDs in the IL. This observation is in stark contrast with the earlier studies of the CdTe QD in an aqueous environment in the presence of S^{2-} where rapid corrosion was observed.[17,26]

The photoluminescence spectra of CdTe QDs in [bmim]-[PF_6] in the presence of various quantities of Na_2S are shown in Figure 3. A drastic sulfide salt induced quenching of the emission of CdTe QDs is likely due to the scavenging of the hole of photoexcited CdTe by a well-known hole scavenger, a sulfide ion,[17,26] and as can be seen from the energetics of the system (Figure 4), the hole transfer process is thermodynamically feasible.

The time-resolved fluorescence behavior of the QDs in the absence and in the presence of various quantities of Na_2S is studied by monitoring the decay profiles at 560 nm. The emission intensity versus time profiles (Figure S1, Supporting Information) were fitted to a triexponential function of the form, $I(t) = a_1 \exp(-t/\tau_1) + a_2 \exp(-t/\tau_2) + a_3 \exp(-t/\tau_3)$, to obtain the decay parameters, which are presented in Table 1, along with the average lifetime $<\tau_a>$, defined by $(a_1\tau_1 + a_2\tau_2 + a_3\tau_3)/(a_1 + a_2 + a_3)$. The measured decay parameters of the QDs in the absence of S^{2-} are in good agreement with the literature.[40−42] On the basis of the literature, the short (1 ns) and the long (∼29 ns) lifetime components are believed to be due to the involvement of deep and shallow trap states, respectively, in carrier recombination,[40] the ∼9 ns component to intrinsic recombination of the core states of CdTe QDs.[43,44]

The emission quenching of CdTe QDs in [bmim][PF_6], as evident from both steady-state and time-resolved studies, is in

dx.doi.org/10.1021/jp507271t | J. Phys. Chem. C 2014, 118, 18481−18487

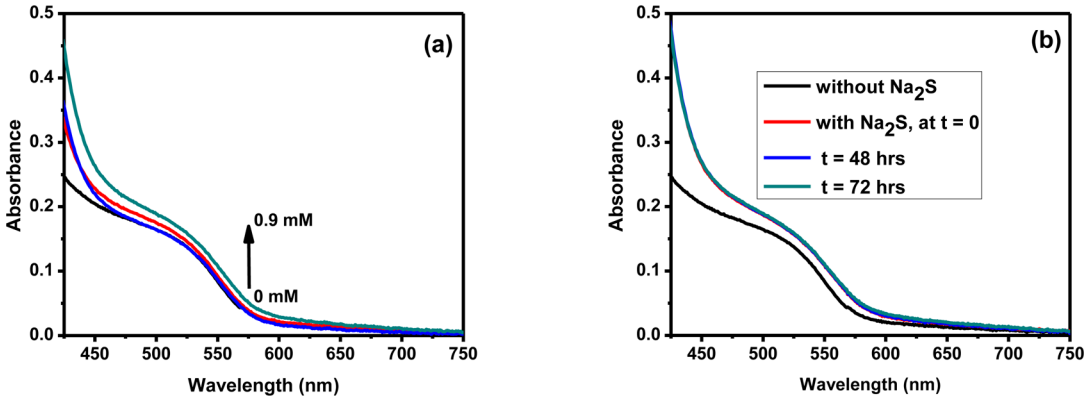

Figure 2. (a) Absorption spectra of CdTe QDs in [bmim][PF_6] with increasing concentration of Na_2S (0, 0.3, 0.6, and 0.9 mM). (b) Absorption spectra of the CdTe QDs in [bmim][PF_6] before and after addition of 0.9 mM Na_2S at different times.

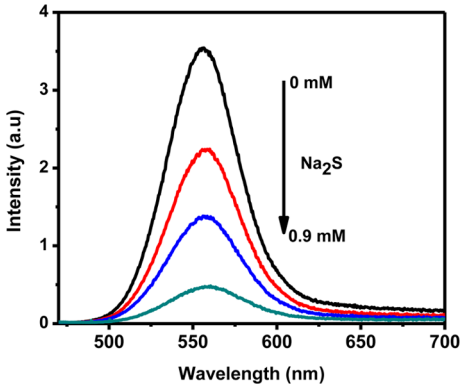

Figure 3. Photoluminescence spectra of CdTe QDs in [bmim][PF_6] with increasing concentration of Na_2S (0, 0.3, 0.6, and 0.9 mM). λ_{exc} = 439 nm.

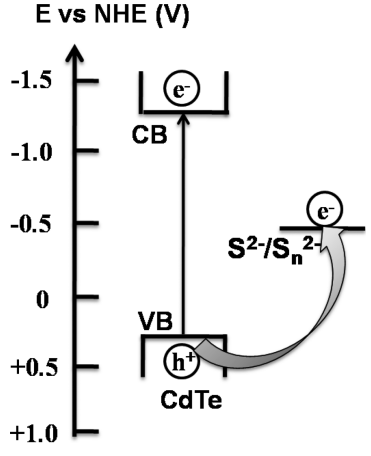

Figure 4. Energy diagram of bulk conduction band (CB) and valence band (VB) potentials of CdTe and reduction potential of S^{2-}/S_n^{2-} (vs NHE). The bulk conduction, valence band potential of CdTe QDs, and reduction potential of sulfide/polysulfide are measured to be at −1.25, + 0.25, and −0.5 V (vs NHE), respectively.[17,26] One should note that, for highly confined CdTe QDs, the actual separation between the VB and the CB levels is much larger than what is shown here.

contrast to the observation made in aqueous environment.[17] Kamat and co-workers observed an increase in the $<\tau_a>$ value of the CdTe QDs on addition of Na_2S in aqueous solution.[17] Interestingly, for CdSe QDs, they observed a decrease of the $<\tau_a>$ value in the presence of Na_2S and attributed it to the hole transfer between a photoexcited CdSe QD and sulfide ion.[17] On the basis of the similarity of this finding with ours, we attribute the decrease of the $<\tau_a>$ value of CdTe QDs with increasing concentration of sulfide ion in [bmim][PF_6] to the scavenging of the holes of photoexcited CdTe QDs by S^{2-}. The fact that, in the presence of 0.9 mM Na_2S, the observed quenching (~85%) of the steady-state fluorescence intensity is considerably higher than that evident from the lifetime data implies that a significant contribution of the quenching comes from the static interaction between the quenching partners.

Table 1. Fluorescence Decay Parameters[a] and Estimated $<\tau_a>$ of the CdTe QDs in [bmim][PF_6]

Na_2S (mM)	τ_1 (a_1)	τ_2 (a_2)	τ_3 (a_3)	$<\tau_a>$
0	9.10 (0.40)	29.66 (0.27)	1.59 (0.33)	12.17
0.3	7.79 (0.36)	25.63 (0.28)	1.23 (0.36)	10.42
0.6	7.00 (0.44)	24.09 (0.23)	0.99 (0.33)	8.95
0.9	6.92 (0.40)	23.80 (0.20)	0.94 (0.40)	7.91

[a]The lifetime values are expressed in ns; these values are accurate within ±0.13 ns.

3.2. Ultrafast Transient Absorption Measurements.

The time-resolved difference absorption spectra of CdTe QDs in [bmim][PF_6] at indicated time delays following 370 nm excitation are shown in Figure 5. The spectra are characterized by a strong bleach centered at 510 nm and a transient absorption in the 530−580 nm region. The bleach around 500−510 nm, which corresponds to the first exciton absorption band of the system (Figure 1), is clearly due to CdTe $\xrightarrow{h\nu}$ CdTe*(e + h) transition. The positive absorption in the 540−580 nm region arises due to the trapped carriers.[45]

In the presence of S^{2-} (Figure 5), the bleach portion of the spectrum disappears completely and a strong absorption covering almost the entire region with two well-defined peaks at around 430 and 570 nm and a dip in the 500−510 nm region at the early time scale is observed. The spectra level off into a broad positive absorption at longer time scales. As the CdTe QD excitonic transition bleach around 500−510 nm is recovered within 70 ps (panel (a) of Figure 5), the dip in the positive absorption in the presence of S^{2-} at early times is due to both broad positive absorption and the CdTe QD excitonic bleach, where the latter contribution disappears at longer time scales.

dx.doi.org/10.1021/jp507271t | J. Phys. Chem. C 2014, 118, 18481−18487

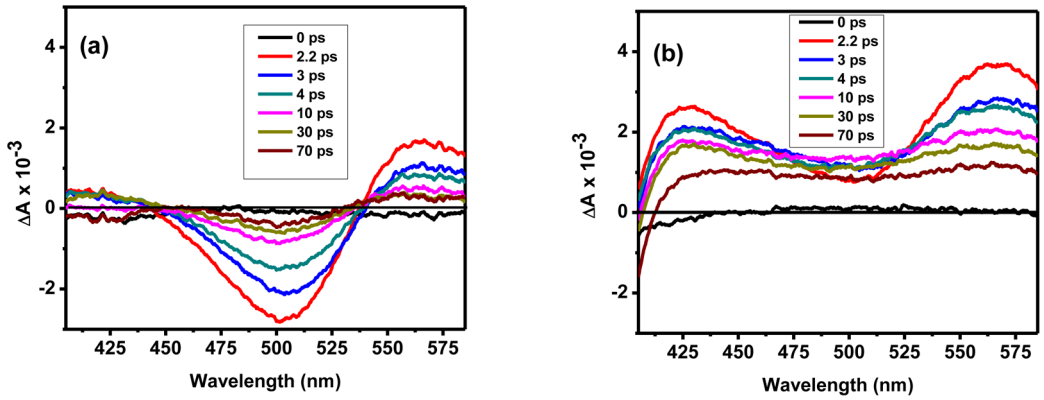

Figure 5. Transient absorption spectra of CdTe QDs (4 μM) in [bmim][PF_6] in the (a) absence and (b) presence of Na_2S (2.7 mM) at different delay times after 370 nm excitation.

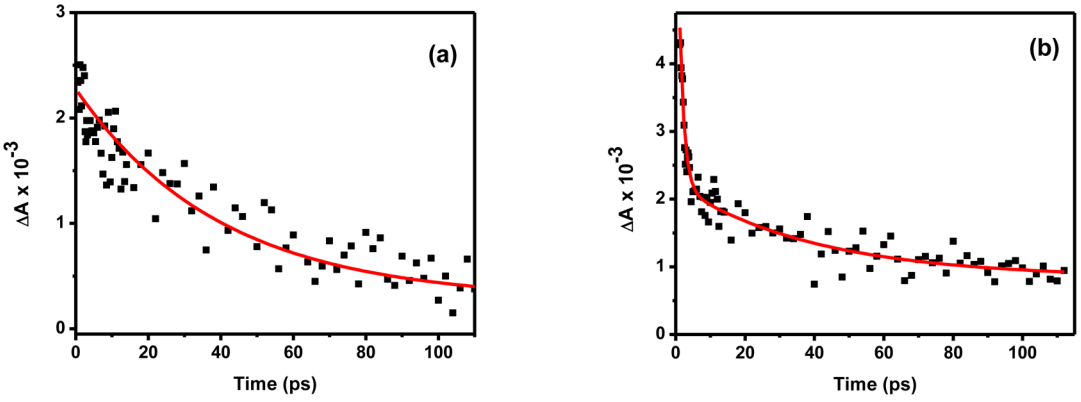

Figure 6. Transient absorption decay kinetics of CdTe QDs (4 μM) in [bmim][PF_6] in the presence of Na_2S (2.7 mM) at 430 nm (a) and 580 nm (b).

In the event of scavenging of the photogenerated hole of CdTe QD by S^{2-}, one expects formation of $S^{-\bullet}$ and various polysulfide radicals according to the following reaction scheme.

$$\mathrm{CdTe} \xrightarrow{h\nu} \mathrm{CdTe^*(e + h)} \quad (1)$$

$$\mathrm{CdTe^*(e + h) + S^{2-} \rightarrow CdTe(e) + S^{-\bullet}} \quad (2)$$

$$\mathrm{S^{-\bullet} + nS^{2-} \rightarrow S_{n+1}{}^{-\bullet}} \quad (3)$$

Considering that the polysulfides absorb in the 400−600 nm region [λ_{max} = 400 nm ($S_2^{-\bullet}$), 580−600 nm ($S_3^{-\bullet}$), and 513 nm ($S_4^{-\bullet}$)], we attribute the absorption around 430 nm to $S_2^{-\bullet}$, 510 nm to $S_4^{-\bullet}$, the one around 570 nm to $S_3^{-\bullet}$.[18,46,47] The bleach due to excitonic transition could not be observed around 510 nm in the presence of S^{2-} due to strong absorption of $S_4^{-\bullet}$.

The absorption due to $S_2^{-\bullet}$ at 430 nm decays rapidly with a time constant of 35 ± 7 ps (Figure 6) in the presence of 2.7 mM S^{2-} primarily due to rapid recombination of $S_2^{-\bullet}$ with CdTe*(e), as illustrated in reaction 4. We do not consider Chakrapani et al.'s observation of a much longer lifetime (few microseconds) of $S_2^{-\bullet}$ surprising as their work was carried out also in the presence TiO_2.[18] The electron CdSe*(e) generated in their case was rapidly injected into TiO_2, and hence, the lifetime of the sulfide radical was determined primarily by the rate of recombination of the electrons in TiO_2 with the $S_{n+1}^{-\bullet}$ (reaction 5).[18]

$$\mathrm{CdTe^*(e) + S_2{}^{-\bullet} \rightarrow CdTe + S_2{}^{2-}} \quad (4)$$

$$\mathrm{TiO_2(e^-) + S_{n+1}{}^{-\bullet} \rightarrow TiO_2 + S_{n+1}{}^{2-\bullet}} \quad (5)$$

The decay kinetics at 580 nm (Figure 6) is found to be biexponential with lifetime components of 1.3 ± 0.2 and 36 ± 8 ps, indicating the presence of two species. As the 530−580 nm absorption in the absence of sulfide salt due to the trapped carriers[45] has a lifetime of 1.3 ± 0.1 ps (Figure S2, Supporting Information), the 36 ps component in the presence of S^{2-} can be attributed to the $S_3^{-\bullet}$ species, which absorbs in this region.[18] The fact that, in the presence of S^{2-}, no long-lived transient species could be observed implies that the various species generated through reactions 1−5 cannot escape out of the cage of the solvent molecules/ions in a viscous IL.

4. CONCLUSION

It is shown that a greater stability to the CdTe nanocrystals can be imparted and the photogenerated holes of the CdTe QDs can be scavenged by S^{2-} employing an ionic liquid as a medium and by appropriate capping of the QDs. The results reported herein seem to provide a route to overcoming some of the drawbacks of an otherwise efficient light harvester and electron injector CdTe nanocrystal that restrict its likely use in quantum-dot-sensitized solar cells.

■ ASSOCIATED CONTENT

Supporting Information

Emission decay profiles of CdTe QDs in [bmim][PF_6] in the absence and presence of Na_2S; transient absorption decay kinetics of CdTe QDs at 580 nm in the absence and presence

dx.doi.org/10.1021/jp507271t | J. Phys. Chem. C 2014, 118, 18481−18487

of Na_2S in [bmim][PF_6]; transient absorption spectra of Na_2S in [bmim][PF_6] at different delay times after 370 nm excitation; absorption and emission spectra of CdTe QDs in $CHCl_3$; photoluminescence spectra of CdTe QDs in [bmim][PF_6] in the absence and presence of methanol; and transient absorption decay parameters of CdTe QDs in [bmim][PF_6]. This material is available free of charge via the Internet at http://pubs.acs.org.

AUTHOR INFORMATION

Corresponding Author

*E-mail: anunay@uohyd.ac.in.

Present Address

†Department of Chemical Physics, Weizmann Institute of Science, Rehovot-76100, Israel

Notes

The authors declare no competing financial interest.

ACKNOWLEDGMENTS

This work is supported by the J. C. Bose Fellowship (to A.S.) of the Department of Science and Technology (DST). The femtosecond pump−probe facility is supported by the University Grants Commission (UGC). Thanks are due to the Council of Scientific and Industrial Research (CSIR) for Fellowships to M.C.S., K.S., J.P.K., N.M., and S.S.

REFERENCES

(1) Nayak, P. K.; Garcia-Belmonte, G.; Kahn, A.; Bisquert, J.; Cahen, D. Photovoltaic Efficiency Limits and Material Disorder. *Energy Environ.* **2012**, *5*, 6022−6039.

(2) Hagfeldt, A.; Boschloo, G.; Sun, L.; Kloo, L.; Pettersson, H. Dye-Sensitized Solar Cells. *Chem. Rev.* **2010**, *110*, 6595−6663.

(3) Jensen, R. A.; Ryswyk, H. V.; She, C.; Szarko, J. M.; Chen, L. X.; Hupp, J. T. Dye-Sensitized Solar Cells: Sensitizer-Dependent Injection into ZnO Nanotube Electrodes. *Langmuir* **2010**, *26*, 1401−1404.

(4) Yu, W. W.; Qu, L.; Guo, W.; Peng, X. Experimental Determination of the Extinction Coefficient of CdTe, CdSe, and CdS Nanocrystals. *Chem. Mater.* **2003**, *15*, 2854−2860.

(5) Buhbut, S.; Itzhakov, S.; Oron, D.; Zaban, A. Quantum Dot Antennas for Photoelectrochemical Solar Cells. *J. Phys. Chem. Lett.* **2011**, *2*, 1917−1924.

(6) Hodes, G. Comparison of Dye- and Semiconductor-Sensitized Porous Nanocrystalline Liquid Junction Solar Cells. *J. Phys. Chem. C* **2008**, *112*, 17778−17787.

(7) Hod, I.; Gonzalez-Pedro, V.; Tachan, Z.; Fabregat-Santiago, F.; Mora-Sero, I.; Bisquert, J.; Zaban, A. Dye versus Quantum Dots in Sensitized Solar Cells: Participation of Quantum Dot Absorber in the Recombination Process. *J. Phys. Chem. Lett.* **2011**, *2*, 3032−3035.

(8) Kamat, P. V. Quantum Dot Solar Cells. Semiconductor Nanocrystals as Light Harvesters. *J. Phys. Chem. C* **2008**, *112*, 18737−18753.

(9) Nozik, A. J. Quantum Dot Solar Cells. *Physica E* **2002**, *14*, 115−120.

(10) Kamat, P. V.; Tvrdy, K.; Baker, D. R.; Radich, J. G. Beyond Photovoltaics: Semiconductor Nanoarchitecutres for Liquid-Junction Solar Cells. *Chem. Rev.* **2010**, *110*, 6664−6688.

(11) Nozik, A. J.; Beard, M. C.; Luther, J. M.; Law, M.; Ellingson, R. J.; Johnson, J. C. Semiconductor Quantum Dots and Quantum Dot Arrays and Applications of Multiple Exciton Generation to Third-Generation Photovoltaic Solar Cells. *Chem. Rev.* **2010**, *110*, 6873−6890.

(12) Kamat, P. V. Quantum Dot Solar Cells. The Next Big Thing in Photovoltaics. *J. Phys. Chem. Lett.* **2013**, *4*, 908−918.

(13) Pan, Z. X.; Zhao, K.; Wang, J.; Zhang, H.; Feng, Y. Y.; Zhong, X. H. Near Infrared Absorption of $CdSe_xTe_{1-x}$ Alloyed Quantum Dot Sensitized Solar Cells with More than 6% Efficiency and High Stability. *ACS Nano* **2013**, *7*, 5215−5222.

(14) Lee, J. W.; Son, D. Y.; Ahn, T. K.; Shin, H. W.; Kim, I. Y.; Hwang, S. J.; Ko, M. J.; Sul, S.; Han, H.; Park, N. G. Quantum-Dot-Sensitized Solar Cell with Unprecedentedly High Photocurrent. *Sci. Rep.* **2013**, *3*, 1050.

(15) Wang, J.; Mora-Sero, I.; Pan, Z.; Zhao, K.; Zhang, H.; Feng, Y.; Yang, G.; Zhong, X.; Bisquert, J. Core/Shell Colloidal Quantum Dot Exciplex States for the Development of Highly Efficient Quantum-Dot-Sensitized Solar Cells. *J. Am. Chem. Soc.* **2013**, *135*, 15913−15922.

(16) Semonin, O. E.; Luther, J. M.; Choi, S.; Chen, H. Y.; Gao, J.; Nozik, A. J.; Beard, M. C. Peak External Photocurrent Quantum Efficiency Exceeding 100% via MEG in a Quantum Dot Solar Cell. *Science* **2011**, *334*, 1530−1533.

(17) Bang, J. H.; Kamat, P. V. Quantum Dot Sensitized Solar Cells. A Tale of Two Semiconcductor Nanocrystals: CdSe and CdTe. *ACS Nano* **2009**, *3*, 1467−1476.

(18) Chakrapani, V.; Baker, D.; Kamat, P. V. Understanding the Role of the Sulfide Redox Couple (S^{2-}/S_n^{2-}) in Quantum Dot-Sensitized Solar Cells. *J. Am. Chem. Soc.* **2011**, *133*, 9607−9615.

(19) Robel, I.; Kuno, M.; Kamat, P. V. Size-Dependent Electron Injection from Excited CdSe Quantum Dots into TiO_2 Nanoparticles. *J. Am. Chem. Soc.* **2007**, *129*, 4136−4137.

(20) Jovanovski, V.; Gonzalez-Pedro, V.; Gimenez, S.; Azaceta, E.; Cabanero, G.; Grande, H.; Tena-Zaera, R.; Mora-Sero, I.; Bisquert, J. A Sulfide/Polysulfide-Based Ionic Liquid Electrolyte for Quantum Dot-Sensitized Solar Cells. *J. Am. Chem. Soc.* **2011**, *133*, 20156−20159.

(21) Yang, Y.; Rodríguez-Córdoba, W.; Lian, T. Ultrafast Charge Separation and Recombination Dynamics in Lead Sulfide Quantum Dot−Methylene Blue Complexes Probed by Electron and Hole Intraband Transitions. *J. Am. Chem. Soc.* **2011**, *133*, 9246−9249.

(22) Bae, W. K.; Joo, J.; Padilha, L. A.; Won, J.; Lee, D. C.; Lin, Q.; Koh, W.; Luo, H.; Klimov, V. I.; Pietryga, J. M. Highly Effective Surface Passivation of PbSe Quantum Dots through Reaction with Molecular Chlorine. *J. Am. Chem. Soc.* **2012**, *134*, 20160−20168.

(23) Nazeeruddin, M. K.; Angelis, F. D.; Fantacci, S.; Selloni, A.; Viscardi, G.; Liska, P.; Ito, S.; Takeru, B.; Gratzel, M. G. Combined Experimental and DFT-TDDFT Computational Study of Photoelectrochemical Cell Ruthenium Sensitizers. *J. Am. Chem. Soc.* **2005**, *127*, 16835−16847.

(24) Tisdale, W. A.; Williams, K. J.; Timp, B. A.; Norris, D. J.; Aydil, E. S.; Zhu, X. Y. Hot-Electron Transfer from Semiconductor Nanocrystals. *Science* **2010**, *328*, 1543−1547.

(25) Schokley, W.; Queisser, H. J. Detailed Balance Limit of Efficiency of p-n Junction Solar Cells. *J. Appl. Phys.* **1961**, *32*, 510−519.

(26) Ellis, A. B.; Kaiser, S. W.; Bolts, J. M.; Wrighton, M. S. Study of n-Type Semiconducting Cadmium Chalcogenide-Based Photoelectrochemical Cells Employing Polychalcogenide Electrolytes. *J. Am. Chem. Soc.* **1977**, *99*, 2839−2848.

(27) Seddon, K. R. *Ionic Liquids: Industrial Applications for Green Chemistry*; American Chemical Society: Washington, DC, 2002.

(28) Dubreuil, J. F.; Bourahla, K.; Rahmouni, M.; Bazureau, J. P.; Hamelin, J. Catalysed Esterifications in Room Temperature Ionic Liquids with Acidic Counteranion as Recyclable Reaction Media. *Catal. Commun.* **2002**, *3*, 185−190.

(29) Hallett, J. P.; Welton, T. Room-Temperature Ionic Liquids: Solvents for Synthesis and Catalysis. 2. *Chem. Rev.* **2011**, *111*, 3508−3576.

(30) Armand, M.; Endres, F.; MacFarlane, D. R.; Ohno, H.; Scrosati, B. Ionic-Liquid Materials for the Electrochemical Challenges of the Future. *Nat. Mater.* **2009**, *8*, 621−629.

(31) Lewandowski, A.; Swiderska-Mocek, A. Ionic Liquids as Electrolytes for Li-Ion Batteries—An Overview of Electrochemical Studies. *J. Power Sources* **2009**, *194*, 601−609.

(32) Gorlov, M.; Kloo, L. Ionic Liquid Electrolytes for Dye-Sensitized Solar Cells. *Dalton Trans.* **2008**, 2655−2666.

(33) Wang, P.; Klein, C.; Humphry-Baker, R.; Zakeeruddin, S. M.; Grätzel, M. Stable ⩾8% Efficient Nanocrystalline Dye-Sensitized Solar

Cell Based on an Electrolyte of Low Volatility. *Appl. Phys. Lett.* **2005**, *86*, 123508.
(34) Santhosh, K.; Samanta, A. Exploring the CdTe Quantum Dots in Ionic Liquids by Employing a Luminescent Hybrid of the Two. *J. Phys. Chem. C* **2012**, *116*, 20643−20650.
(35) Santhosh, K.; Banerjee, S.; Rangaraj, N.; Samanta, A. Fluorescence Response of 4-(*N*,*N*′-Dimethylamino)benzonitrile in Room Temperature Ionic Liquids: Observation of Photobleaching under Mild Excitation Condition and Multiphoton Confocal Microscopic Study of the Fluorescence Recovery Dynamics. *J. Phys. Chem. B* **2010**, *114*, 1967−1974.
(36) Perrin, D. D.; Armerego, W. L. F.; Perrin, D. R. *Purification of Laboratory Chemicals*; Pergaman Press: New York, 1980.
(37) Wuister, S. F.; Swart, I.; Driel, F. V.; Hickey, S. G.; Donega, D. D. M. Highly Luminescent Water-Soluble CdTe Quantum Dots. *Nano Lett.* **2003**, *3*, 503−507.
(38) Santhosh, K.; Samanta, A. Modulation of the Excited State Intramolecular Electron Transfer Reaction and Dual Fluorescence of Crystal Violet Lactone in Room Temperature Ionic Liquids. *J. Phys. Chem. B* **2010**, *114*, 9195−9200.
(39) Banerjee, S.; Pabbathi, A.; Sekhar, M. C.; Samanta, A. Dual Fluorescence of Ellipticine: Excited State Proton Transfer from Solvent versus Solvent Mediated Intramolecular Proton Transfer. *J. Phys. Chem. A* **2011**, *115*, 9217−9225.
(40) Fitzmorris, B. C.; Cooper, J. K.; Edberg, J.; Gul, S.; Guo, J.; Zhang, J. Z. Synthesis and Structural, Optical, and Dynamic Properties of Core/Shell/Shell CdSe/ZnSe/ZnS Quantum Dots. *J. Phys. Chem. C* **2012**, *116*, 25065−25073.
(41) Santhosh, K.; Patra, S.; Soumya, S.; Khara, D. C.; Samanta, A. Fluorescence Quenching of CdS Quantum Dots by 4-Azetidinyl-7-nitrobenz-2-oxa-1,3-diazole: A Mechanistic Study. *ChemPhysChem* **2011**, *12*, 2735−2741.
(42) Boulesbaa, A.; Huang, Z.; Wu, D.; Lian, T. Competition between Energy and Electron Transfer from CdSe QDs to Adsorbed Rhodamine B. *J. Phys. Chem. C* **2010**, *114*, 962−969.
(43) Klimov, V. I.; McBranch, D. W.; Leatherdale, C. A.; Bawendi, M. G. Electron and Hole Relaxation Pathways in Semiconductor Quantum Dots. *Phys. Rev. B: Condes. Matter Mater. Phys.* **1999**, *60*, 13740−13749.
(44) Wang, X.; Qu, L.; Zhang, J.; Peng, X.; Xiao, M. Surface-Related Emission in Highly Luminescent CdSe Quantum Dots. *Nano Lett.* **2003**, *3*, 1103−1106.
(45) Rawalekar, S.; Kaniyankandy, S.; Verma, S.; Ghosh, H. N. Ultrafast Charge Carrier Relaxation and Charge Transfer Dynamics of CdTe/CdS Core−Shell Quantum Dots as Studied by Femtosecond Transient Absorption Spectroscopy. *J. Phys. Chem. C* **2010**, *114*, 1460−1466.
(46) Chivers, T.; Drummond, I. Characterization of the Trisulfur Radical Anion S_3^- in Blue Solutions of Alkali Polysulfides in Hexamethylphosphoramide. *Inorg. Chem.* **1972**, *11*, 2525−2527.
(47) Clark, R. J. H.; Cobbold, D. G. Characterization of Sulfur Radical Anions in Solutions of Alkali Polysulfides in Dimethylformamide and Hexamethylphosphoramide and in the Solid State in Ultramarine Blue, Green, and Red. *Inorg. Chem.* **1978**, *17*, 3169−3174.